

①

A222 810

---

# Effects of Small-Scale Heterogeneities on Regional Propagation

---

S. Flatté

March 1990

JSR-89-151

Approved for public release; distribution unlimited.

**DTIC**  
**SELECTE**  
**JUN 19 1990**  
**S B D**

JASON  
The MITRE Corporation  
7525 Colshire Drive  
McLean, Virginia 22102-3481  
(703) 883-6997

## REPORT DOCUMENTATION PAGE

Form Approved  
OMB No 0704-0188  
Exp Date Jun 30, 1986

1a REPORT SECURITY CLASSIFICATION <b>UNCLASSIFIED</b>			1b RESTRICTIVE MARKINGS <b>NONE</b>		
2a SECURITY CLASSIFICATION AUTHORITY <b>N/A SINCE UNCLASSIFIED</b>			3 DISTRIBUTION/AVAILABILITY OF REPORT Approved for public release; distribution unlimited.		
2b DECLASSIFICATION/DOWNGRADING SCHEDULE <b>N/A SINCE UNCLASSIFIED</b>					
4 PERFORMING ORGANIZATION REPORT NUMBER(S) <b>JSR-89-151</b>			5 MONITORING ORGANIZATION REPORT NUMBER(S) <b>JSR-89-151</b>		
6a NAME OF PERFORMING ORGANIZATION <b>JASON Program Office The MITRE Corporation</b>		6b OFFICE SYMBOL (if applicable) <b>A10</b>	7a NAME OF MONITORING ORGANIZATION <b>DARPA</b>		
6c ADDRESS (City, State, and ZIP Code) <b>7525 Colshire Drive McLean, VA 22102-3481</b>			7b ADDRESS (City, State, and ZIP Code) <b>1400 Wilson Boulevard Arlington, VA 22209-2308</b>		
8a NAME OF FUNDING/SPONSORING ORGANIZATION <b>DARPA</b>		8b OFFICE SYMBOL (if applicable) <b>T10</b>	9 PROCUREMENT INSTRUMENT IDENTIFICATION NUMBER		
8c ADDRESS (City, State, and ZIP Code) <b>1400 Wilson Boulevard Arlington, VA 22209-2308</b>			10. SOURCE OF FUNDING NUMBERS		
			PROGRAM ELEMENT NO	PROJECT NO <b>8503Z</b>	TASK NO WORK UNIT ACCESSION NO
11 TITLE (Include Security Classification) <b>Effects of Small Scale Heterogeneities on Regional Propagation</b>					
12 PERSONAL AUTHOR(S) <b>Stanley M. Flatte</b>					
13a TYPE OF REPORT <b>Technical</b>		13b TIME COVERED FROM _____ TO _____		14 DATE OF REPORT (Year, Month, Day) <b>90/01/21</b>	15 PAGE COUNT <b>25</b>
16 SUPPLEMENTARY NOTATION					
17 COSATI CODES			18 SUBJECT TERMS (Continue on reverse if necessary and identify by block number) <b>propagation; heterogeneities; seismic-wave, crustal waveguide.</b>		
FIELD	GROUP	SUB-GROUP			
19 ABSTRACT (Continue on reverse if necessary and identify by block number) <b>Regional seismic-wave propagation at frequencies above 1 Hz is described in terms of ray theory, and the effects of small-scale heterogeneities are described statistically by means of the modern theory of wave propagation through random media. Observed features of regional propagation, such as the complexity of waveforms over tens or hundreds of seconds, the sensitivity of this complexity to the location of source or receiver, and the spread in arrival angles of waves at a receiving array, are explained by this propagation model.</b>					
20 DISTRIBUTION/AVAILABILITY OF ABSTRACT <input checked="" type="checkbox"/> UNCLASSIFIED/UNLIMITED <input type="checkbox"/> SAME AS RPT <input type="checkbox"/> DTIC USERS			21 ABSTRACT SECURITY CLASSIFICATION <b>UNCLASSIFIED</b>		
22a NAME OF RESPONSIBLE INDIVIDUAL <b>Dr. Robert G. Henderson</b>			22b TELEPHONE (Include Area Code) <b>(703) 883-6997</b>	22c OFFICE SYMBOL <b>JASON Prog Ofc</b>	

## Abstract

Regional seismic-wave propagation at frequencies above 1 Hz is described in terms of ray theory, and the effects of small-scale heterogeneities are described statistically by means of the modern theory of wave propagation through random media. Observed features of regional propagation, such as the complexity of waveforms over tens or hundreds of seconds, the sensitivity of this complexity to the location of source or receiver, and the spread in arrival angles of waves at a receiving array, are explained by this propagation model.

<b>Accession For</b>	
NTIS GRA&I	<input checked="" type="checkbox"/>
DTIC TAB	<input type="checkbox"/>
Unannounced	<input type="checkbox"/>
Justification	
By _____	
Distribution/	
Availability Codes	
Dist	Avail and/or Special
A-1	

SEARCHED  
SERIALIZED  
INDEXED

# Contents

<b>1 INTRODUCTION</b>	<b>1</b>
<b>2 CRUSTAL WAVEGUIDE PROPAGATION</b>	<b>5</b>
<b>3 THE EFFECTS OF HETEROGENEITIES</b>	<b>9</b>
3.1 Fluctuation Regime . . . . .	10
3.2 Intensity Fluctuations . . . . .	12
3.3 Time Spread . . . . .	13
3.4 Angular Spread . . . . .	14
3.5 Averaging and Calibration Distances . . . . .	15
<b>4 DISCUSSION AND CONCLUSIONS</b>	<b>17</b>

# 1 INTRODUCTION

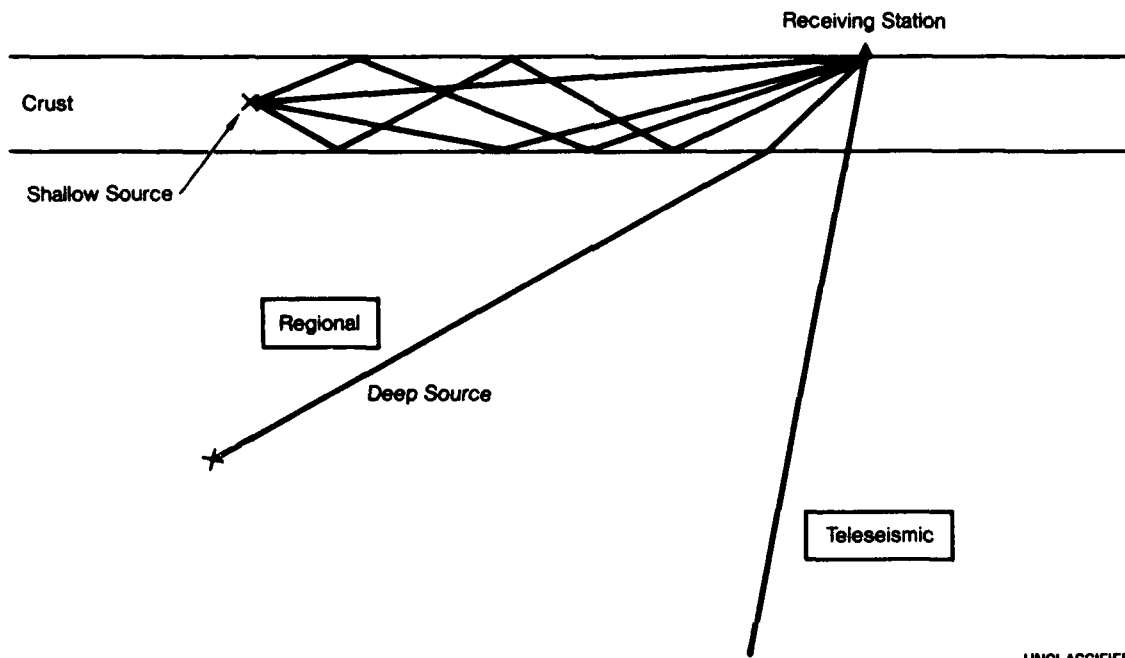
Seismic waves travelling over regional distances (100-1000 km) from shallow sources must travel through the crustal waveguide. There have been many studies of this type of propagation, and a number of attempts to explain its behavior in terms of models of earth structure. Some explanations have concentrated on the details of horizontally stratified wavespeed structure, with the wave equation being solved in terms of normal modes.<sup>1</sup> Other explanations have used ray theory as a starting point.<sup>2</sup> Most of these analyses have modelled earth structure in a deterministic manner; that is, models were presented that defined the seismic wavespeed exactly for every point in space.

For seismic waves above 1 Hz, a number of recent studies have analysed waveform variability in terms of a statistical model of earth heterogeneities. Teleseismic P-wave amplitude and arrival-time fluctuations have been explained on the basis of heterogeneities in the lithosphere and upper mantle; these studies were sensitive to heterogeneities with rms wavespeed variations of a few percent and horizontal scale lengths from a few kilometers to tens of kilometers.<sup>3</sup> These teleseismic waves come up toward the receiver stations with angles not too far from the zenith. (See Figure 1.) Propagation over regional distances from deep earthquakes (well below the crust) has also been analysed in terms of heterogeneities, and similar results have been obtained.<sup>4</sup>

In both the above studies, the model of deterministic propagation, before the addition of heterogeneities, was a very simple one; it consisted of incident straight-line rays, or plane waves.

It is the purpose of this study to analyse regional propagation from shallow sources from the same point of view as the above studies. For this purpose we must make a simple model of deterministic propagation in the absence of heterogeneities; this is done in Section 2. Then the effects of heterogeneities are added in Section 3. We will see that this statistical approach explains many of the features of regional propagation.

Our simple model consists of a constant-depth crustal waveguide with a constant wavespeed, overlying a uniform half-space with a constant (higher)



UNCLASSIFIED

**Figure 1.** Schematic of the arrival of seismic waves at a receiver on the earth's surface, for a simple deterministic model of earth structure involving the crustal waveguide. Waves from near the zenith come nearly straight through; they represent teleseismic arrivals. Waves from sources that are below the crustal waveguide are refracted slightly, but still have a single, well-defined ray as a deterministic model of the propagation. Waves from sources within the crustal waveguide can reflect many times on their way to a receiver.

wavespeed. A real region of the crust will be more complicated than our simple model, even disregarding small-scale heterogeneities. For example, the depth of the waveguide may be variable with geographical position, or the wavespeed may have a small gradient, or a series of step changes within the waveguide. We will see that when we add the heterogeneities, the complexity introduced into the received waveforms is so drastic, that if we had started with a more complicated deterministic model, it would not have qualitatively changed our conclusions.

In this study we will ignore the problem of conversion between compressional and shear waves. Our study may be thought of as initially applying to SH propagation, since there is no conversion of SH waves in our deterministic model. Again, the variations introduced by the heterogeneities are so significant, even for pure SH waves, that our qualitative conclusions will probably apply in general, but this is clearly an area deserving of further first-order study.

## 2 CRUSTAL WAVEGUIDE PROPAGATION

Deterministic propagation in the crustal waveguide at high frequencies can be analysed from the point of view of ray theory. Our model will be a uniform-speed waveguide of thickness  $h$  and wavespeed  $\beta$ , with a uniform-speed half-space underlying it. The speed in the underlying medium will be designated  $\beta_2$ . We will take a source at depth  $d$  at a distance  $R$  from a receiver station on the surface. (See Figure 2.)

The solution to our simple model is straightforward, and consists of a sequence of straight-line rays that are reflected  $n$  times from the surface or bottom of the waveguide, where  $n$  is  $0, \pm 1, \pm 2 \dots$  up to a maximum determined by critical reflection at the bottom of the waveguide. This critical reflection angle is determined by the ratio of the wavespeeds in the two regions of the earth:

$$\cos \Theta_{\text{critical}} < \beta/\beta_2.$$

Let  $\Theta_n$  be the angle of the  $n$ th ray with the horizontal. The requirement that  $\Theta_n < \Theta_{\text{critical}}$  can be more usefully expressed by the equation:

$$|d + 2nh| < [(\beta_2/\beta)^2 - 1]^{1/2} R.$$

The number of rays  $N$  can be expressed approximately from this equation:

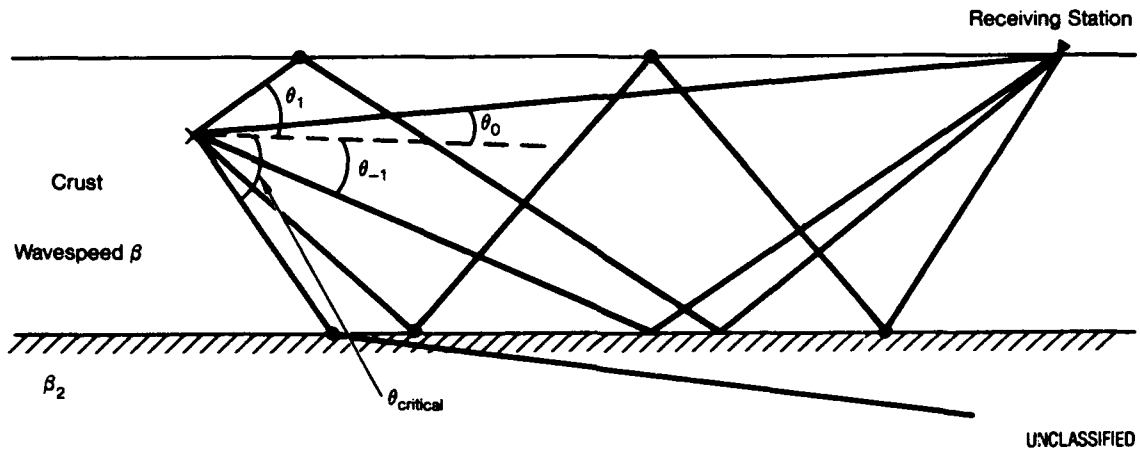
$$N = (R/h) [(\beta_2/\beta)^2 - 1]^{1/2}.$$

The intensity of each ray can be calculated from simple spherical spreading, because each ray can be unwrapped from its reflections into a simple straight line having a length of  $R/\cos \Theta_n$ . Therefore, the intensity of the  $n$ th ray is:

$$I_n = S(\Theta_n) \cos^2 \Theta_n / R^2 = S(\Theta_n) / [R^2 + (d + 2nh)^2]$$

where  $S(\Theta_n)$  is the angular distribution at the source. From here on we will assume for simplicity that the source is isotropic; that is,  $S(\Theta_n) = 1$ . If we normalize the intensity pattern by having the first ray (with  $n=0$ ) have





UNCLASSIFIED

**Figure 2.** Diagram of rays from a source in the crustal waveguide to a receiver on the surface. Each ray has an angle  $\theta_n$  with the horizontal. The wavespeeds in the crustal waveguide and below are  $\beta$  and  $\beta_2$ , respectively. Rays with angles above the critical angle get lost in the deep earth.

an intensity of unity, then it is easy to show that the last ray will have the minimum intensity, and it will be

$$I_{\min} = (\beta/\beta_2)^2$$

The arrival time of each ray is easily calculated from the distance travelled ( $R/\cos\Theta_n$ ):

$$t_n = (R/\beta) \left\{ 1 + [(d + 2nh)/R]^2 \right\}^{1/2}.$$

Note that if  $d \ll h$ , then the two rays corresponding to positive and negative  $n$  come in very close together; there is a twinning of arrivals associated with the source and its image reflected in the earth's surface. The patterns that result for several ranges of propagation in a crustal waveguide with realistic average values for the various characteristic parameters are shown in Figure 3.

It is useful to calculate the approximate spacing between the discrete arrivals for later comparison with the effects of heterogeneities. Let  $\Delta t_n$  be the spacing between the  $n$ th and  $(n+1)$ th rays:

$$\Delta t_n = (2h/\beta)\xi_n/[1 + \xi_n^2]^{1/2}$$

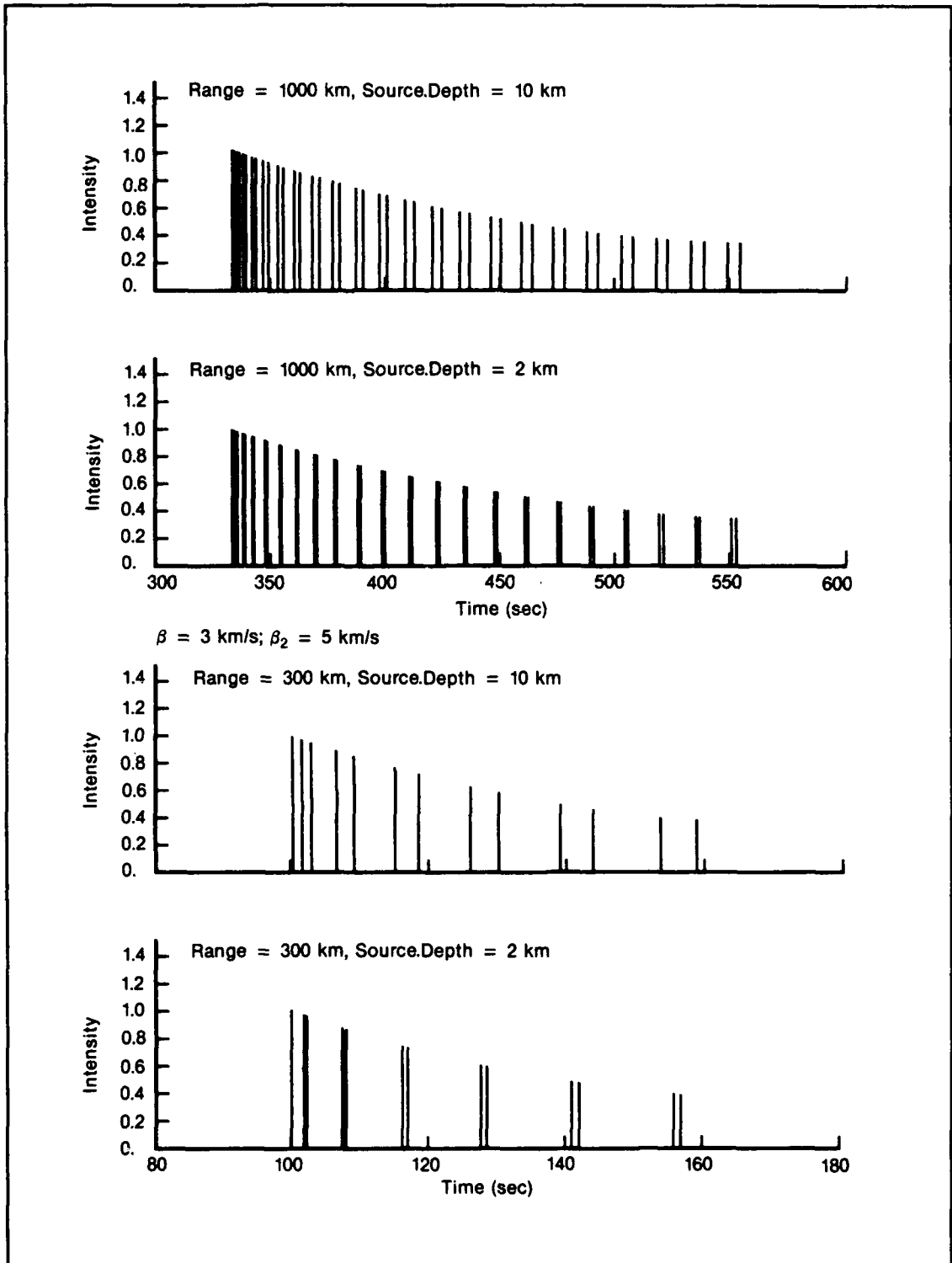
where

$$\xi_n = |(d + 2nh)/R|.$$

This expression does not account for the twinning due to positive and negative  $n$ . It is of interest to note that near the first arrival, the separation is much smaller than near the last arrival:

$$\begin{aligned} \Delta t_1 &= (2h/\beta)(2h/R) \\ \Delta t_{\max} &= (2h/\beta). \end{aligned}$$

For example, if  $h=30$  km,  $R=600$  km, and  $\beta = 3$  km/s, then  $\Delta t_1 = 2$  s and  $\Delta t_{\max} = 20$  s.



UNCLASSIFIED

**Figure 3. (U)** Examples of expected high-frequency waveforms for our simple deterministic crustal waveguide parameters, with no heterogeneities. The plots are for two different ranges (300 km and 1000 km) and two different source depths (2 km and 10 km). The parameters of the crust are:  $h=30 \text{ km}$ ,  $\beta=3 \text{ km/s}$ , and  $\beta_2=5 \text{ km/s}$ .

### 3 THE EFFECTS OF HETEROGENEITIES

The simple arrival structure described in Section 2 is not observed experimentally. The arrival pattern is more complex, with intensity as a function of time being an apparently random jumble that begins about where the first arrival is expected, and continues until dying away in the noise many tens of seconds later.

We will calculate the effect of small-scale heterogeneities on our deterministic arrival structure by use of the path-integral theory of wave propagation through random media, developed in large part for the case of acoustic propagation in the ocean.<sup>5-11</sup> To begin with, we need a statistical model for the heterogeneities. For the purpose of this illustrative study, we will take an anisotropic Gaussian correlation function with scale lengths in the horizontal ( $L_V$ ) and vertical ( $L_H$ ) and an rms fractional variation in wavespeed of  $\mu$ .

We emphasize that we are taking a simplistic picture of the medium in assuming that it is composed of the superposition of two disparate structures: First, a very simple deterministic structure (a plane layer over a homogeneous half-space), and second, small-scale random velocity perturbations in the crustal layer. Other effects, which are certainly of importance in specific regions, might be topography on the surfaces of the crustal layer, or reflecting surfaces within the crust. The point of our study is that much of what is actually observed may often be explained by random volume velocity perturbations, so that such perturbations should not be ignored in a first-order explanation of observations, particularly at high frequency.

We will take the values of velocity-fluctuation quantities from the studies that have been carried out on teleseismic waves arriving at large arrays, and from recent studies of regional propagation from deep earthquakes. The relation between crustal-waveguide propagation and teleseismic effects is dependent on the anisotropy of the medium fluctuations, which is not well known. We are only giving order-of-magnitude examples here; in the study of a specific geographical region, careful consideration to specific anisotropy models should be given.

Typical values of these fluctuation quantities, from the teleseismic study and the study of regional propagation from deep earthquakes, might be:  $\mu \sim 2\%$ ,  $L_V \sim 5$  km, and  $L_H \sim 10$  km. However, the results are quite sensitive to the exact choices of values, and to the particular spectrum chosen. Therefore, a more quantitative study must be done to compare with actual data from a specific geographical region.

### 3.1 Fluctuation Regime

Various regimes of wave fluctuation behavior were identified in Reference 5 and 6, and quantities were defined that are necessary for determining the regime in which a particular situation lies. These quantities are:

- The strength parameter  $\Phi$ , which is the rms phase that a wave would experience if it travelled exactly along the deterministic ray. This would be the actual rms phase only if the heterogeneities were weak enough, but even when the heterogeneities are strong, the calculation of the strength parameter is crucial to the wave-fluctuation analysis.
- The diffraction parameter  $\Lambda$ , which is the square of the ratio between the size of the Fresnel zone and the transverse correlation length of the medium, averaged over the deterministic ray. Small diffraction parameter means that diffraction is small, so that the concepts of generalized geometrical optics are quite useful. Large diffraction parameter means that diffraction is very important; in this situation concepts of uncorrelated multiple scatter are probably useful.
- The various regimes in  $\Lambda - \Phi$  space are shown in Figure 4. We need to define a few more quantities in order to calculate these parameters. They are:
- The wavenumber of the propagating seismic wave, which we will denote by  $q$ . For example, a 1-Hz shear wave travelling in a crust with a speed of 3.14 km/s has a wavenumber  $q = 2 \text{ km}^{-1}$ .

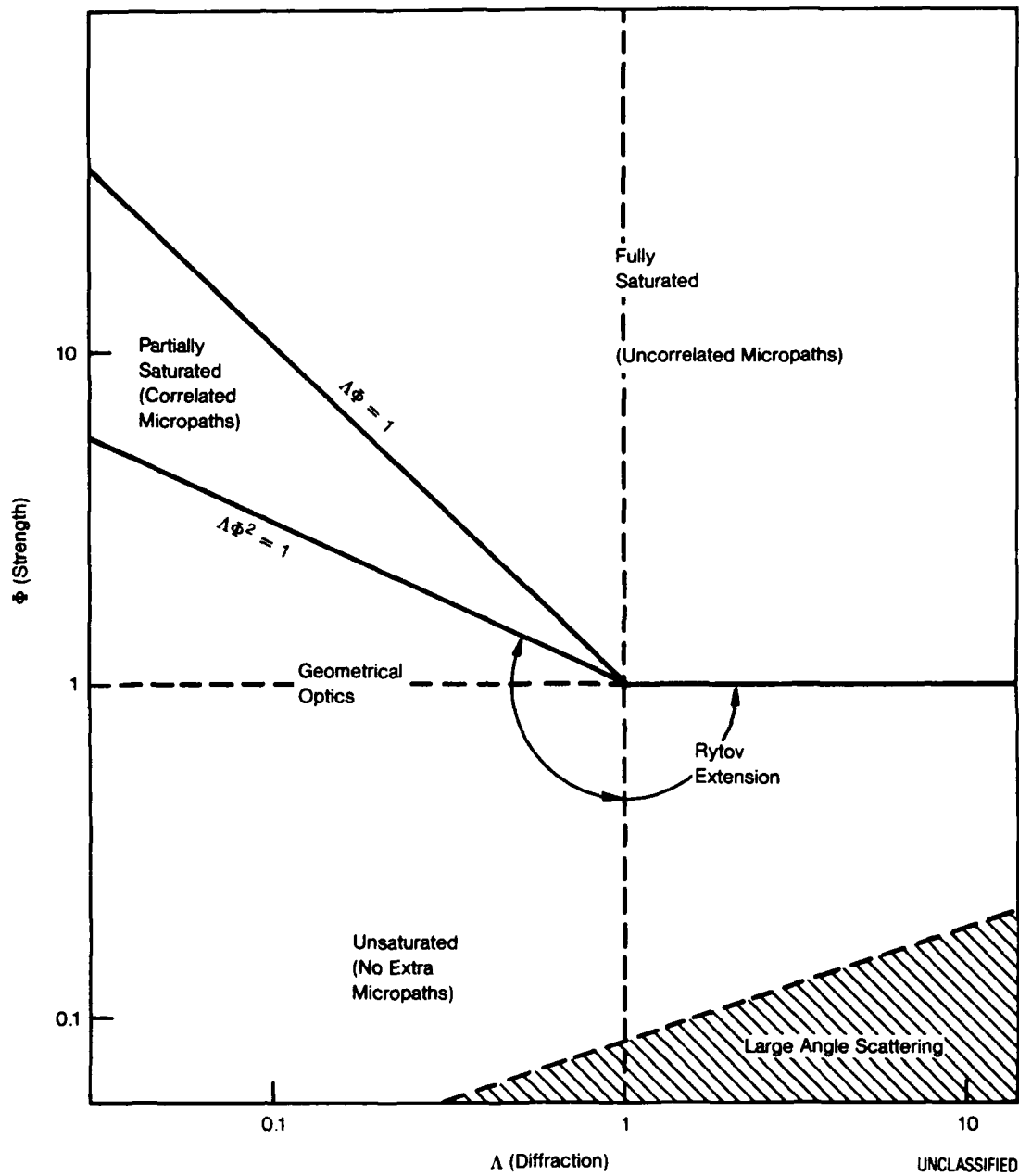


**Figure 4.**  $\Lambda$ - $\Phi$  diagram showing the different regimes of wave fluctuation behavior for waves propagating through random media (from Reference 6).

- The parallel ( $L_P$ ) and transverse ( $L_T$ ) correlation length of the medium, where parallel means along the deterministic ray, and transverse means perpendicular to the deterministic ray. In an anisotropic medium, these can often be expressed in terms of  $L_V$  and  $L_H$ .

In terms of defined quantities, the following results for the strength and diffraction parameters follow:

$$\begin{aligned}\Phi^2 &= q^2 \mu^2 L_P R = 16 \\ \Lambda &= R / (6qL_T^2) = 3.3 \\ \Lambda \Phi^2 &= (1/6)q\mu^2 R^2 L_P / L_T^2 = 53 \\ \Lambda \Phi &= (1/6)\mu R(L_P R)^{1/2} / L_T^2 = 13\end{aligned}$$

and putting in our so-called typical numbers yields the numerical values indicated, for a propagation range of 1000 km.

The fact that both  $\Lambda \Phi$  and  $\Phi$  are greater than unity tells us that we are in full saturation. In this regime we have many uncorrelated microrays; that is, each deterministic ray is broken up by the heterogeneities into many rays. This remains true as one moves to higher frequency.

### 3.2 Intensity Fluctuations

In the fully saturated regime, the intensity of a given ray, at least at a single frequency, is Rayleigh distributed. That means that the intensity has a simple exponential distribution function. As long as the analysis is being done on a limited frequency band that does not exceed the coherent bandwidth, the result is that each of the arrivals in, for example, Figure 3, will have an intensity taken from this exponential distribution function, with mean value given by the deterministic result. However, as will be shown below, the case of interest here has a very small coherent bandwidth. In that case, the observation can be thought of as being within a small interval of time, so small that the time spread of the received pulse is much larger than the observation interval, and the intensity within each observation time interval will be a random variable with a large variance.

### 3.3 Time Spread

In the fully saturated regime, a delta-function pulse emitted by the source is spread in time by an amount given by<sup>5</sup>

$$\tau_n = \Lambda\Phi^2/(q\beta) \{1 + \xi_n^2\}.$$

We can compare this spread to the separation between the deterministic arrivals by taking the ratio of the two:

$$\tau_n/\Delta t_n = \Lambda\Phi^2/(2qh)[1 + \xi_n^2]^{3/2}/\xi_n.$$

The  $\xi_n$  at small  $n$  are small compared with unity (on the order of  $h/R$ ), and rise to a maximum of

$$\xi_{\max} = [(\beta_2/\beta)^2 - 1]^{1/2}.$$

A few simple substitutions of numerical values reveals that the ratio of  $\tau/\Delta t$  is always greater than unity. Thus the spread due to heterogeneities is always larger than the separation between deterministic arrivals, resulting in a waveform that essentially appears to be random.

For example, for our typical numbers at 1000 km range, we find that

$$\begin{aligned}\tau_1 &= 9s \\ \tau_N &= 25s\end{aligned}$$

and we see that in all cases the spread fills in any gaps one might have observed in the deterministic propagation.

The coherent bandwidth of the propagation is the inverse of the time spread. The numbers above imply that the coherent bandwidth is in the range of 0.04-0.10 Hz.



### 3.4 Angular Spread

In the fully saturated regime, the energy that starts from a point source and arrives at a point receiver has travelled within a spatial region that is determined by the medium fluctuations rather than the finite wavelength of the seismic wave. The size of this spatial region also determines the spread in arrival angle of the energy as it arrives at the receiver.

The determination of this angular spread is dependent on a function known as the phase structure function, which is the variance of phase difference between two nearby rays that start from the source and end near the receiver with a small separation  $x$ . In the case of a Gaussian correlation function, the phase structure function  $D$  is given by

$$D(x) = \Phi^2(x/L_T)^2.$$

The rms angular spread is determined by the value of  $x$  (call it  $x_o$ ) at which  $D(x_o)=1$ . Thus:

$$x_o = L_T/\Phi$$

and

$$\Theta_{\text{rms}} = 1/(x_o q) = \Phi/(qL_t).$$

For our typical case, in which  $\Phi = 4$ ,  $q = 2 \text{ km}^{-1}$ , and  $L_T = 5 \text{ km}$ , we have  $\Theta_{\text{rms}} = 0.4$  radians, or  $23^\circ$ . Note that the angular spread scales with the square root of range, and is independent of frequency.

Thus, an array that attempts to determine the location of the source by beamforming will find that the inherent inaccuracy due to the heterogeneities has a standard deviation on the order of  $20^\circ$  at 1000 km.

### 3.5 Averaging and Calibration Distances

The distance  $x_o$  represents the distance over which the arriving wave field is decorrelated. Therefore, if one wants to go back and verify the exact waveform received in a particular event by repeating the transmission by some means, then one must place both the source and the receiver within a fraction of  $x_o$  of the original transmission. This would be true for both the horizontal and vertical position. In our typical case, the value of  $x_o$  is about 1 km.

By the same token, if one were attempting to average out the effects of heterogeneities, one would get approximately independent samples every  $x_o$ , and therefore many receivers spaced by that distance would give a good average.

However, this conclusion is really not accurate for media that are multiscale rather than Gaussian. We would expect that the larger averaging region would be affected by larger-scale medium variations, and the variance would not go down proportionally to the number of receiving stations. This kind of calculation can be done for any given model of medium fluctuations.

## 4 DISCUSSION AND CONCLUSIONS

An intuitive understanding of regional propagation of high frequency seismic waves for sources that lie within the crustal waveguide has been presented in terms of a very simple deterministic propagation model combined with the effects of small-scale heterogeneities. Our simple deterministic model implies that the underlying pattern of arrivals is a series of sharp arrivals associated with the multiray structure expected in a waveguide. Reasonable numerical values for heterogeneities in the crust yield very significant effects on the received arrivals. These effects include variations in amplitude, arrival time, and arrival angle. As a result of these fluctuations, the received waveforms will lose their detailed connection with the underlying arrival pattern, and will become a jumble of arrivals whose spread in time overlaps with the nearby deterministic arrivals. The variations in intensity of each arrival caused by the heterogeneities are large.

The angular spread of the arriving energy can be calculated, and for 1000-km propagation has an rms value of  $20^\circ$  or more. This angular spread also implies that nearby receivers will not be coherent with each other at distances comparable to 1 km, and that the use of calibration shots of some kind in order to measure the propagation from a particular source to a particular receiver must be done under the limitation that the calibration shot must be within that 1-km distance.

## REFERENCES

1. B.L.N. Kennett, Lg-Wave Propagation in Heterogeneous Media, Final Report, 15 Feb. 1988-14 Feb. 1989, GL-TR-89-0102.
2. R.W. Clayton, D.G. Harkrider, and D.V. Helmberger, Modeling Regional Seismic Waves from Underground Nuclear Explosion, Scientific Report No. 1, 9 May, 1988, AFGL-TR-88-0135.
3. S.M. Flatté and R.S. Wu, J. Geophys. Res. 93, 6601 (1988).
4. H. Sato, Broadening of Seismogram Envelopes in the Randomly Inhomogeneous Lithosphere Based on the Parabolic Approximation: Southeast Honshu, Japan, J. Geophys. Res., in press (1989).
5. S.M. Flatté et al, Sound Transmission through a Fluctuating Ocean, Cambridge University Press, New York (1979).
6. S.M. Flatté, PROC. IEEE, 71, 1267-1294 (1983).
7. R. Dashen, S.M. Flatté, and S.A. Reynolds, J. Acoust. Soc. Am. 77, 1718 (1985).
8. S.A. Reynolds et al, J. Acoust. Soc. Am. 77, 1723 (1985).
9. S.M. Flatté, S.A. Reynolds, and R. Dashen, J. Acoust. Soc. Am. 82, 967 (1987).
10. S.M. Flatté et al, J. Acoust. Soc. Am. 82, 973 (1987).
11. S.M. Flatté and R. Stoughton, J. Acoust. Soc. Am. 84, 1414 (1988).

*DISTRIBUTION LIST*

Dr. Henry D.I. Abarbanel  
Institute for Nonlinear Science  
Mail Code R002/Building CMRR/Room 115  
University of California/San Diego  
La Jolla, CA 92093-0402

Dr. Ralph W. Alewine III  
Director  
Nuclear Monitoring Research Office  
DARPA/NMRO  
1400 Wilson Boulevard  
Arlington, VA 22209-2308

Dr. Marvin C. Atkins [3]  
Deputy Director  
Science and Technology  
Defense Nuclear Agency  
6801 Telegraph Road  
Alexandria, VA 22310

The Honorable John A. Betti  
Undersecretary of Defense for Acquisition  
The Pentagon, Room 3E933  
Washington, DC 20301-3000

Dr. Arthur E. Bisson  
Technical Director of Submarine  
and SSBN Security Program  
Department of the Navy, OP-02T  
The Pentagon, Room 4D534  
Washington, DC 20350-2000

Dr. Robert R. Blandford  
DARPA/NMRO  
1400 Wilson Boulevard  
Arlington, VA 22209-2308

Mr. Edward C. Brady  
Sr. Vice President and General Manager  
The MITRE Corporation  
Mail Stop Z605  
7525 Colshire Drive  
McLean, VA 22102

The Honorable D. Allan Bromley  
Asst to the President for Science and  
Technology  
Office of Science and Technology Policy  
Old Executive Office Building, Room 360  
17th & Pennsylvania Avenue, N.W.  
Washington, DC 20506

Mr. Edward Brown  
DARPA/PM  
1400 Wilson Boulevard  
Arlington, VA 22209-2308

Dr. Herbert L. Buchanan, III  
Director  
DARPA/DSO  
1400 Wilson Boulevard  
Arlington, VA 22209-2308

Dr. Kenneth M. Case  
Institute for Nonlinear Science  
Mail Code R-002  
University of California/San Diego  
San Diego, CA 92093-0402

Dr. Ferdinand N. Cirillo, Jr.  
Central Intelligence Agency  
Washington, DC 20505

*DISTRIBUTION LIST*

Mr. John Darrah  
Senior Scientist and Technical Advisor  
HQAF SPACOM/CN  
Peterson AFB, CO 80914-5001

Dr. Russ E. Davis  
Scripps Institution of Oceanography  
A-030  
University of California/San Diego  
La Jolla, CA 92093

DTIC [2]  
Defense Technical Information Center  
Cameron Station  
Alexandria, VA 22314

Professor Freeman J. Dyson  
Institute for Advanced Study  
Olden Lane  
Princeton, NJ 08540

Maj Gen Robert D. Eaglet  
Assistant Deputy SAF/AQ  
The Pentagon, Room 4E969  
Washington, DC 20330-1000

Dr. Douglas M. Eardley  
Institute for Theoretical Physics  
University of California  
Santa Barbara, CA 93106

Mr. John N. Entzminger  
Director  
DARPA/TTO  
1400 Wilson Boulevard  
Arlington, VA 22209-2308

Dr. Craig I. Fields  
Director  
DARPA  
1400 Wilson Boulevard  
Arlington, VA 22209-2308

Dr. Stanley M. Flatte  
Physics Department  
Natural Sciences II  
University of California  
Santa Cruz, CA 95064

Dr. Robert Foord [2]  
Central Intelligence Agency  
Washington, DC 20505

Dr. Norval Fortson  
Department of Physics  
FM-15  
University of Washington  
Seattle, WA 98195

Dr. Larry Gershwin  
Central Intelligence Agency  
Washington, DC 20505

*DISTRIBUTION LIST*

Dr. David Gifford  
Central Intelligence Agency  
Washington D.C., 20505

Dr. S. William Gouse  
Sr. Vice President and General Manager  
The MITRE Corporation  
Mail Stop Z605  
7525 Colshire Drive  
McLean, VA 22102

Dr. Michael C. Gregg  
Applied Physics Laboratory  
1013 N.E. 40th Street  
Seattle, WA 98105

LTGEN Robert D. Hammond  
Commander and Program Executive Officer  
U.S. Army / CSSD-ZA  
Strategic Defense Command  
P.O. Box 15280  
Arlington, VA 22215-0150

Dr. William Happer  
Department of Physics  
Princeton University  
Box 708  
Princeton, NJ 08544

MAJGEN Jerry C. Harrison  
Commander  
U.S. Army Laboratory Command  
2800 Powder Mill Road  
Adelphi, MD 20783-1145

Dr. Robert G. Henderson  
Director  
JASON Program Office  
The MITRE Corporation  
7525 Colshire Drive, Z561  
McLean, VA 22102

Mr. James V. Hirsch  
Central Intelligence Agency  
Washington, DC 20505

Dr. Paul Horowitz  
Lyman Laboratory of Physics  
Harvard University  
Cambridge, MA 02138

JASON Library [5]  
The MITRE Corporation  
Mail Stop: W002  
7525 Colshire Drive  
McLean, VA 22102

Dr. O'Dean P. Judd  
Chief Scientist  
Strategic Defense Initiative Organization  
Room 1E1083  
The Pentagon  
Washington, DC 20301-7100

Dr. Jonathan I. Katz  
Department of Physics  
Washington University  
St. Louis, MO 63130

*DISTRIBUTION LIST*

Dr. Herbert Levine  
Department of Physics  
Mayer Hall/B019  
University of California/San Diego  
La Jolla, CA 92093

Dr. Gordon MacDonald  
The MITRE Corporation  
Mail Stop Z605  
7525 Colshire Drive  
McLean, VA 22102

Mr. Robert Madden [2]  
Department of Defense  
National Security Agency  
ATTN: R-9 (Mr. Madden)  
Ft. George G. Meade, MD 20755-6000

Mr. Charles R. Mandelbaum  
U.S. Department of Energy  
Code ER-32  
Mail Stop: G-236  
Washington, DC 20545

Mr. Arthur F. Manfredi, Jr.  
OSWR  
Central Intelligence Agency  
Washington, DC 20505

Dr. Claire E. Max  
Inst. of Geophysics & Planetary Physics  
Lawrence Livermore Natl Lab  
L-413  
P.O. Box 808  
Livermore, CA 94550

LtGen George L. Monahan, Jr.  
Director/SDIO-D  
Strategic Defense Initiative Organization  
The Pentagon  
Washington, DC 20301-7100

MGEN Thomas S. Moorman, Jr.  
Director of Space and SDI Programs  
Code SAF/AQS  
The Pentagon  
Washington, DC 20330-1000

Dr. Richard A. Muller  
Lawrence Berkeley Laboratory  
Building 50/Room 232  
Berkeley, CA 94720

Dr. Walter H. Munk  
University of California/San Diego  
Scripps Institution of Oceanography  
A-025  
La Jolla, CA 92093

Dr. Julian C. Nall  
Institute for Defense Analyses  
1801 North Beauregard Street  
Alexandria, VA 22311

Dr. William A. Nierenberg  
Director Emeritus  
Scripps Institution of Oceanography  
A021  
University of California/San Diego  
La Jolla, CA 92093



*DISTRIBUTION LIST*

Dr. Robert L. Norwood [2]  
Acting Director for Space  
and Strategic Systems  
Office of the Assistant Secretary of the Army  
The Pentagon, Room 3E374  
Washington, DC 20310-0103

Mr. Gordon Oehler  
Central Intelligence Agency  
Washington, DC 20505

Dr. Peter G. Pappas  
Chief Scientist  
U.S. Army Strategic Defense Command  
P.O. Box 15280  
Arlington, VA 22215-0280

Mr. Jay Parness  
Central Intelligence Agency  
Washington, DC 20505

Dr. Allen M. Peterson  
Space, Telecommunications & Radioscience  
Lab  
Department of Electrical Engineering  
227 Durand Building/Stanford University  
Stanford, CA 94305

MAJ Donald R. Ponikvar  
Strategic Defense Command  
Department of the Army  
P.O. Box 15280  
Arlington, VA 22215-0280

Mr. John Rausch [2]  
NAVOPINTCEN Detachment, Suitland  
4301 Suitland Road  
Washington, DC 20390

Records Resources  
The MITRE Corporation  
Mailstop: W115  
7525 Colshire Drive  
McLean, VA 22102

Dr. Victor H. Reis  
Deputy Director  
DARPA  
1400 Wilson Boulevard  
Arlington, VA 22209-2308

Dr. Carl Romney  
Center for Seismic Studies  
1300 N. 17th Street, Suite 1415  
Arlington, VA 22209-3871

Dr. Malvin A. Ruderman  
Department of Physics  
Columbia University  
New York, NY 10027

Dr. Fred E. Saalfeld  
Director  
Office of Naval Research  
800 North Quincy Street  
Arlington, VA 22217-5000

*DISTRIBUTION LIST*

BGEN Anson Schulz  
Acting Deputy Director  
Strategic Defense Initiative Organization  
1E1081  
The Pentagon  
Washington, DC 20301

Dr. Philip A. Selwyn [2]  
Director  
Office of Naval Technology  
800 North Quincy Street  
Arlington, VA 22217-5000

The Honorable Michael P.W. Stone  
Secretary of the Army  
Washington, DC 20310-0101

Dr. Jeremiah D. Sullivan  
237C Loomis Laboratory of Physics  
University of Illinois/Urbana-Champaign  
1110 West Green Street  
Urbana, IL 61801

Superintendent  
Code 1424  
Attn: Documents Librarian  
Naval Postgraduate School  
Monterey, CA 93943

Dr. Vigdor Teplitz  
ACDA/SPSA  
320 21st Street, N.W.  
Room 4923  
Washington, DC 20451

Dr. Sam B. Treiman  
Physics Department  
Princeton University  
Princeton, NJ 08540

Ms. Michelle Van Cleave  
Assistant Director for National Security  
Affairs  
Office of Science and Technology Policy  
New Executive Office Building  
17th and Pennsylvania Avenue  
Washington, DC 20506

Mr. Richard Vitali  
Director of Corporate Laboratory  
U.S. Army Laboratory Command  
2800 Powder Mill Road  
Adelphi, MD 20783-1145

Dr. Kenneth M. Watson  
Marine Physical Laboratory  
Scripps Institution of Oceanography  
University of California/Mail Code P-001  
San Diego, CA 92152

Mr. Robert Williams  
Chief of Advanced Technology  
DARPA  
1400 Wilson Boulevard  
Arlington, VA 22209-2308

RADM (Sel) Ray Witter  
Director - Undersea Warfare  
Space and Naval Warfare Systems Command  
Code: PD-80  
Department of the Navy  
Washington, DC 20363-5100

***DISTRIBUTION LIST***

**RADM Daniel J. Wolkenstorfer  
Director  
DASWD (OASN/RD&A)  
The Pentagon  
Room 5C676  
Washington, DC 20350-1000**

**Dr. Herbert F. York  
IGCC (D-018)  
University of California/San Diego  
La Jolla, CA 92093**

**Dr. Fredrik Zachariasen  
California Institute of Technology  
452-48  
1201 East California Street  
Pasadena, CA 91125**

**Mr. Charles A. Zraket  
President and Chief Executive Officer  
The MITRE Corporation  
Mail Stop A265  
Burlington Road  
Bedford, MA 01730**